

**Instrumentation and Measurement Strategy for the NOAA SENEX
Aircraft Campaign as Part of the Southeast Atmosphere Study 2013**

Supplementary information:

Detailed descriptions of instruments on the NOAA WP-3D

1. Aerosol Particle Size Distributions: PI Charles Brock

The NOAA ESRL cloud and aerosol processes group operated three instruments that together provided the concentration of particles as a function of their dry size from 0.004 μm to 7.0 μm diameter. The size distribution is a fundamental property of the atmospheric aerosol, and it contributes to understanding aerosol sources and sinks, optical properties, cloud nucleation potential, and chemical transformations.

Particles with diameters from ~ 0.004 to 0.07 μm were measured with a 5-channel condensation particle counter (CPC), the nucleation-mode aerosol size spectrometer (NMASS) (Brock et al., 2000). This unique instrument samples particles into a low pressure region (~ 100 hPa) where they are exposed to a warm vapor from a perfluorinated organic compound. The sample airstream is then cooled, producing a supersaturation of the vapor. Particles larger than a critical size are nucleated form a droplet of the organic fluid and are counted with a simple laser optical counter. Each of the five NMASS channels operates at a different temperature, so that the critical diameter varies in each. Particles with diameters larger than 0.004, 0.008, 0.015, 0.030, and 0.055 μm are nucleated and counted independently. Differencing the channels provides a coarse resolution, but fast (1 second) time response, measurement of the size distribution of ultrafine particles.

Particles with diameters from 0.07 to ~ 1.0 μm were measured by an ultra-high sensitivity aerosol spectrometer (UHSAS) (Brock et al., 2011). The aerosol sample enters a resonant cavity that is driven by a solid-state laser at 1053 nm wavelength. The size of each particle is determined by measuring the amount of

side-scattered light reaching two solid-state photodiode detectors. The instrument was housed in the same rack as the aerosol optical properties (AOP) instruments, and sampled from the same dried (<10% relative humidity, RH) airstream that supplied the optical instruments. The UHSAS has been substantially modified from the commercial laboratory version (Droplet Measurement Technologies, Boulder, Colorado) and has been equipped with an RH control system. The RH of the sample can be switched between the default dry mode and an elevated humidity (~85% RH). The change in the aerosol size distribution can be used to evaluate the hygroscopicity of the particles. The humidified and dry size distribution can be used to calculate how aerosol properties, such as directional scattering (asymmetry parameter) vary with atmospheric humidity.

Particles with diameters from ~0.7 μm to 7.0 μm were measured with a custom-built white-light optical particle counter (WLOPC). This instrument detects light from a 3-watt white-light-emitting diode (LED) source that is scattered over a wide angle by single particles. The white light source is used to reduce particle sizing biases caused by widely varying particle compositions and shapes that are typical of supermicron aerosol particles. The high sample flow rate of the WLOPC results in acceptable counting statistics for supermicron particles over time periods of ~10 s at typical coarse particle concentrations. The inlet of the WLOPC is maintained at <40% RH by heating the sample line as necessary.

The UHSAS and WLOPC operated in the WP-3D cabin and sampled air downstream of the low-turbulence inlet (LTI) (Wilson et al., 2004). The LTI actively removes turbulent flow developing along the walls of a conical diffuser. Since the NMASS measures ultrafine particles subject to diffusive rather than inertial losses, it sampled instead from a double diffusing inlet in a non-pressurized wing pod.

2. Cloud condensation nuclei (CCN): PI Athanasios Nenes

The Georgia Tech group operated a Continuous Flow Streamwise Thermal Gradient CCN chamber (CFSTGC) (Lance et al., 2006; Roberts and Nenes, 2005) in Scanning Flow CCN Analysis mode (SFCA) (Moore and Nenes, 2009) on the WP-3D

during the SENEX mission. The instrument provided CCN spectra, or the number of aerosol that act as cloud condensation nuclei as a function of supersaturation.

The CFSTGC used is made by Droplet Measurement Technologies (CCN-100, DMT; Lance et al., 2006) and consists of a cylindrical metal tube (0.5 m in length with a 23 mm inner diameter and 10 mm wall thickness) with a wetted inner wall on which a linear temperature gradient is applied in the stream-wise direction. The temperature gradient is controlled using three thermoelectric coolers (TECs) located on the outer wall of the flow chamber (Figure S1), and water flows continuously through a 2.5 mm thick, porous, ceramic bisque that lines the inside of the cylinder. Heat and water vapor diffuse toward the centerline of the flow chamber. Since moist air is largely composed of N_2 and O_2 , which are heavier molecules than H_2O , the latter has a higher molecular velocity, hence diffuses more quickly than heat (which is transferred primary via collisions between slower N_2 , O_2). Under developed flow conditions, a quasi-parabolic water vapor supersaturation is generated in the radial direction, which is maximized at the centerline (Roberts and Nenes, 2005). The aerosol sample enters the top of the column at the centerline and is surrounded by a blanket of humidified, aerosol-free sheath air. If the supersaturation in the instrument exceeds the critical supersaturation of the aerosol, the particles activate and form droplets, which are counted and sized by an optical particle counter (OPC) using a 50 mW, 658 nm wavelength laser diode light source. The droplet concentration is then equal to the concentration of CCN at the supersaturation considered. The droplet size distribution information obtained in the OPC also allows using the CFSTGC to study CCN activation kinetics (Raatikainen et al., 2012).

The CFSTGC was operated in Scanning Flow CCN Analysis (SFCA) (Moore and Nenes, 2009) mode, which allowed rapid, high-resolution measurements of CCN spectra. SFCA is based on varying the instrument flow rate while keeping the instrument pressure and streamwise temperature difference constant. Varying the flow rate at a sufficiently slow rate allows the operation of the instrument at “pseudo-steady” state, where instantaneous flow rates correspond to an instantaneous supersaturation and greatly facilitates inversion of the CCN

timeseries to a CCN spectrum. SFCA overcomes the limitations of operating the CFSTGC under a “constant flow” mode (where the flow rate is maintained at a constant value and supersaturation is adjusted by changing the column temperature gradient in the streamwise direction), requiring 20-120 seconds for column temperatures to stabilize during a supersaturation change. During SENEX, CCN spectra were obtained every 30-60 seconds, for a supersaturation range of 0.2 to 1.0%. The CCN concentration uncertainty was $\pm 10\%$, or 5-10 cm^{-3} under conditions of low counting statistics. The absolute supersaturation uncertainty was $\pm 0.04\%$ (Moore et al., 2012).

Supersaturation in the instrument was sensitive to pressure fluctuations associated with altitude changes; for this a DMT pressure control box combined with a custom-built inlet (that minimizes particle losses) was connected upstream of the CFSTGC (Figure S1). The device ensured a constant pressure in the CFSTGC, typically set to a value below the minimum ambient pressure encountered during a science flight.

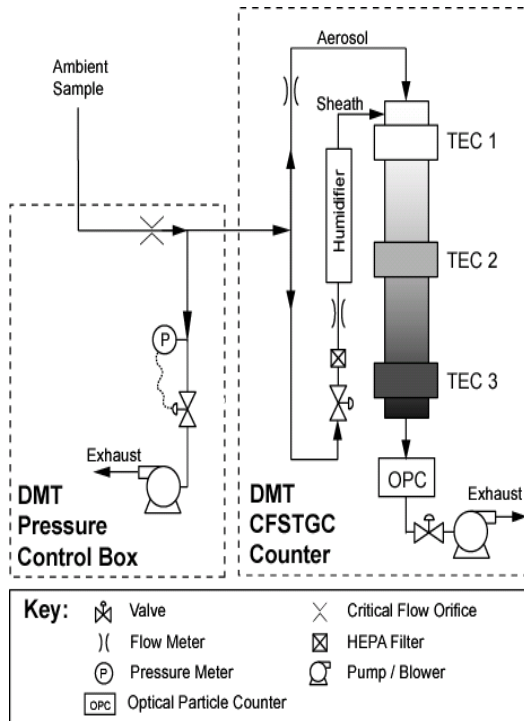


Figure S1: Instrument setup for measuring CCN spectra during SENEX.

3. Aerosol Optical Properties (AOP)

The NOAA ESRL cloud and aerosol processes group operated an aerosol optical properties (AOP) instrument package on the NOAA P3 during the SENEX mission. The AOP package provided multi-wavelength, multi-RH aerosol extinction and absorption measurements with fast response and excellent accuracy and stability on aircraft platforms. The instruments also characterized the optics of black carbon (BC) mixing state, brown carbon, and water uptake of aerosol. Two instruments, a cavity ringdown (CRD) aerosol extinction spectrometer and a photoacoustic absorption spectrometer (PAS) comprised the AOP package.

3.1. Cavity ringdown aerosol extinction spectrometer (CRD): PI Justin Langridge, Nick Wagner

The CRD instrument (Langridge et al., 2011) is composed of 8 separate ringdown cavities (Figure S2). Each channel of the instrument consists of a sample cell located between two highly reflective mirrors, which form an optical cavity with effective path lengths ranging from 7 km to 60 km in particle-free air. A laser is used to periodically inject light into the cavity and the optical power in the cavity decays exponentially after the laser turned off. Light leaking through the back mirror of the cavity is used to monitor the decay. The time constant of the exponential decay is proportional to the total extinction coefficient of the optical cavity. The extinction due to aerosol is measured using the difference in the extinction when aerosol is present or absent from the sample cell. Before entering the sample cell, the aerosol is dried using a nafion drier (Permapure PD-200T-12-MSS, Toms River, New Jersey, USA), and gas-phase absorbers are removed using an activated carbon monolith (MAST Carbon NovaCarb F, Basingstoke, United Kingdom).

Three channels are used to measure dry ($RH < 25\%$) extinction coefficients at 405, 532, and 662 nm. Two channels measure extinction coefficients downstream of 250°C thermal denuder at 405 nm and 662 nm, and two channels measure 532 nm extinction coefficients downstream of nafion humidifiers (Permapure MH-110-12SD-4, Toms River, New Jersey, USA), which are controlled to 70% and 90% RH. An eighth channel measures 405 nm extinction coefficients downstream of a

particle filter, which served as a check for the scrubbing of gas-phase absorbers. The CRD had a 1 Hz sensitivity of 0.1 Mm^{-1} , and accuracy of $<2\%$, and a precision of $\sim 10\%$ for extinctions in the range of $10\text{-}100 \text{ Mm}^{-1}$. The precision is improved to $\sim 1\%$ with sample averaging to 60 s.

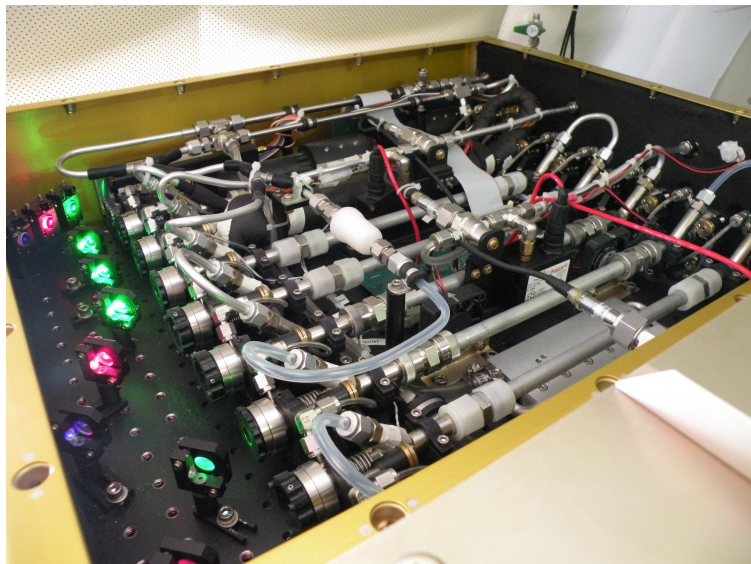


Figure S2: The 8 separate ringdown cells in the CRD instrument

3.2. Photoacoustic absorption spectrometer (PAS): PI Daniel Lack

The PAS instrument (Lack et al., 2012) is composed of 5 separate acoustic resonators that also serve as sample cells that are each illuminated by a multi-pass optical cavity. A continuous-wave laser is intensity-modulated at the acoustic resonance frequency of each resonator. Light-absorbing particles heat the air, producing acoustic pulses that are detected with a sensitive microphone. Because the resonance frequency varies with pressure and temperature, a speaker is used to actively determine the resonance frequency and tune the laser modulation to match. Like the CRD instrument, the PAS samples aerosol downstream of a nafion drier (Permapure PD-200T-12-MSS, Toms River, New Jersey, USA), and gas-phase absorbers are removed using an activated carbon monolith (MAST Carbon NovaCarb F, Basingstoke, United Kingdom).

Three of the channels of the PAS instrument are used to measure dry absorption coefficients at 405, 532 and 662 nm. The remaining two channels measure absorption downstream of the thermal denuder. Accuracy of the PAS is ~10% and sensitivity is $\sim 1 \text{ Mm}^{-1}$ for 1 Hz sampling.

The combined AOP instrument package measured the aerosol properties necessary for calculations of radiative forcing and atmospheric heating rates. Further, the measured parameters can be directly compared to those derived from remote sensing measurements from satellite, airborne, and ground-based sensors. Additional measurements, such as the change in aerosol absorption and extinction as condensed coatings are thermally evaporated from absorbing cores, will improve mechanistic understanding of the role of clear and brown carbon coatings in controlling aerosol optical properties, and the sources and evolution of these coatings in the atmosphere. Finally, the absorption of the refractory cores can be compared to the BC mass measurements, allowing a direct linkage between atmospheric loadings of BC and radiative effects and helping constrain simulations of aerosol impacts on climate.

4. Single-Particle Soot Photometer (SP2): PI Joshua P. Schwarz, Milos Markovic

The SP2 is a laser-induced incandescence instrument that measures the refractory black carbon (rBC) mass content of individual particles and thus delivers detailed information not only about rBC loadings, but also size distributions, even in exceptionally clean air (Schwarz et al., 2010). The instrument can also provide the optical size of individual particles containing rBC and identify the presence of optically significant internal mixtures with the BC fraction (Schwarz et al., 2008). Note that rBC is experimentally equivalent to elemental carbon as measured by OC/EC instruments at the level of 15% (Kondo et al., 2011).

The SP2 system is shown schematically in Figure S3. Ambient air is drawn through an intense intracavity laser (a diode-pumped Nd:YAG laser operating in a Gaussian TEM-00 mode at $1.064 \mu\text{m}$ wavelength). Aerosol particles in the air enter the laser singly and scatter laser light according to their size, composition and

morphology. The quantity of scattered light and its evolution in time are recorded. When an rBC-containing particle enters the laser, the rBC is heated to vaporization ($\sim 3500\text{K}$), emitting blackbody radiation (incandescent light) in the visible in quantities directly related to its mass, regardless of particle morphology or mixing state. The color of this radiation is detected and used to deduce the vaporization temperature of the particle as a constraint on its composition. A detector system developed by NOAA is used to optically size rBC-containing particles before laser heating perturbs them. This allows quantification of the amount of non-BC material (interpreted as a coating thickness via shell-core Mie theory) associated with each BC core, and its impact on the optical properties (including absorption cross-section) of the BC-component. Only a limited range of rBC mass in individual particles can be quantified; this range covers most of the accumulation mode rBC mass that dominates total rBC aerosol loadings, except near tail-pipes.

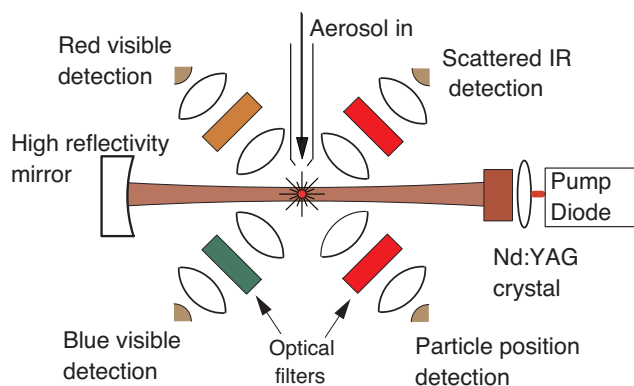


Figure S3. Schematic diagram of the SP2 photometer showing the basic optics and laser-induced incandescence and scattering detectors.

5. Compact-Time-of-Flight Aerosol Mass Spectrometer (C-ToF AMS): PI

Ann Middlebrook, Jin Liao, Andre Welti

A key aspect of the SENEX project was to quantify the abundance and chemical composition of atmospheric aerosol particles above the Southeastern United States. To accomplish this, we use a semi-custom Compact Time-of-Flight

Aerosol Mass Spectrometer or C-ToF-AMS with a light scattering (LS) module (Aerodyne Research Inc., Billerica, MA).

The general operation of AMS instruments has been described elsewhere (Allan et al., 2003; Canagaratna et al., 2007; Jayne et al., 2000; Jimenez et al., 2003). Briefly, particles are transmitted into the AMS detection region using an aerodynamic focusing lens, where they impact an inverted-cone porous-tungsten vaporizer typically held at ~ 600 °C, and volatilize, with the vapors being analyzed by electron ionization mass spectrometry. The C-ToF-AMS system deployed here employs a long aerosol time-of-flight drift region and a compact-time-of-flight mass spectrometer, which combined has high size-resolution and high sensitivity for individual particle mass spectral signals (DeCarlo et al., 2006; Drewnick et al., 2005). Particles between 100 and 700 nm vacuum aerodynamic diameter are sampled with 100% efficiency through the specific aerodynamic focusing lens used here and the custom pressure-controlled inlet designed for airborne operation (Bahreini et al., 2008; Liu et al., 1995). Details on calibration, data collection and data processing are described elsewhere (Allan et al., 2004; Bahreini et al., 2009; Middlebrook et al., 2012). For SENEX, the AMS was operated with low sensitivity, which increased the uncertainty in accuracy to roughly 50%.

The LS module has been previously used by other investigators in a few laboratory and field studies (Cross et al., 2009; Cross et al., 2007; Liu et al., 2012; Slowik et al., 2010). Here it was deployed for the first time on an airborne platform. The LS module consists of a 405 nm, continuous laser beam directed at the end of the aerosol time-of-flight drift region before particles impact on the vaporizer, an ellipsoidal mirror for collecting scattered light from particles passing through the laser beam, and a photomultiplier tube for detecting and measuring the scattered light. The data acquisition software used the scattered light signal to trigger saving mass spectra for that individual particle.

One important factor for particle detection efficiency in the AMS instrument is efficient evaporation after particle impaction on the vaporizer, where inefficient evaporation is commonly referred to as particle “bounce” (Matthew et al., 2008; Middlebrook et al., 2012). To provide a direct measurement of this factor for

ambient aerosols, particles must be large enough to scatter light in the instrument (for the current system ~ 100 nm in diameter), provide enough signal from the single particle mass spectra to detect them, and evaporate in less than a few hundred μ s. The LS module provides a quantitative measure of the particles that are not detected due to “bouncing” on the vaporizer.

6. Carbon Dioxide (CO₂) and Methane (CH₄) (Picarro): PI Jeff Peischl, Thomas Ryerson

Measurements of the greenhouse gases carbon dioxide (CO₂) and methane (CH₄) were used to determine the sources and magnitudes of these emissions in the southeast U.S. during SENEX. CO₂ and CH₄ were measured aboard the WP-3D aircraft using a modified commercial wavelength-scanned cavity ring-down analyzer (Picarro 1301-m) (Peischl et al., 2012). Atmospheric air was sampled through a 3/8 in. OD stainless steel rearward facing inlet on the WP-3D and dried to a dew point temperature of -78°C after passage through a 200-strand Nafion dryer and a dry ice trap. The absorption cell pressure was controlled at 140 Torr (± 0.2 Torr during smooth flight, and ± 0.5 Torr during typical boundary layer flight conditions; all stated uncertainties are $\pm 1\sigma$).

Immediately inside the fuselage, two CO₂ and CH₄ calibration gas standards were regularly added to the inlet line during flight to evaluate instrument sensitivity. The calibration standards bracketed the expected ambient range of each gas and are known to within ± 0.07 ppm CO₂ and ± 1 ppb CH₄ (all CO₂ and CH₄ mixing ratios are reported as dry air mole fractions). The calibration gases were added at a flow rate sufficient to overflow the inlet. These flight standard tanks, or secondary standards, were calibrated before and after the field project using primary CO₂/CH₄ standard tanks tied to the WMO standard scale from the Global Monitoring Division (GMD) at the NOAA Earth System Research Laboratory (ESRL). A third calibration standard (referred to as a “target”) was regularly introduced to the inlet between calibrations and treated as an unknown to evaluate long-term instrument performance.

Independent of the target retrievals, we estimated a total accuracy in the CO₂ measurement of ± 0.10 ppmv and a total accuracy in the CH₄ measurement of ± 1.2 ppbv for 20-second averages. One-second precision of the CO₂ measurement was ± 0.10 ppmv during smooth flight and ± 0.15 ppmv during turbulent flight. One-second precision of the CH₄ measurement was ± 1.5 ppbv during smooth flight and ± 2.0 ppbv during turbulent flight.

7. Carbon Monoxide (CO) and Sulfur Dioxide (SO₂): PI John Holloway

The CO instrument was contained in a pod located on the left wing inboard (Holloway et al., 2000). The instrument consists of a VUV fluorimeter, a vacuum/sample pump, compressed gas cylinders, and a data system and computer. The computer in the wing pod boots when electrical power is supplied to the pod. Data acquisition software starts automatically. Communication with the pod is by means of 100 base T Ethernet. The precision of the measurements is estimated to be 2.5%. Variability in the determination of zero levels results in an absolute uncertainty of about 0.5 ppbv in the values reported. The field standard was compared to NIST Standard Reference Material (SRM) 2612a (10 ppmv nominal CO in air). The concentration of the calibration standard is known to within 2%. The overall accuracy of the 1s measurements is thus estimated to be 5%.

The SO₂ instrument was located in a one bay rack inside the aircraft. It consists of a TECO model 43C pulsed fluorimeter, an external sample pump, a rack mounted computer and associated data system interface box, compressed gas cylinders containing zero air and a 10 ppm SO₂/N₂ calibration standard, and a calibration system mounted on the sample inlet (Ryerson et al., 1998).

8. Nitrogen Oxides and Ozone (NO_y/O₃): PI Ilana Pollack, Thomas Ryerson

The NOAA NO_yO₃ 4-channel chemiluminescence (CL) instrument provided in-situ measurements of nitric oxide (NO), nitrogen dioxide (NO₂), total reactive nitrogen oxides (NO_y), and ozone (O₃) on the WP-3D during SENEX. This instrument has flown on the WP-3D, the NCAR Electra, and the NASA DC-8 research aircraft on multiple field projects since 1995 (Pollack et al., 2010; Ryerson et al., 1999; Ryerson

et al., 2000). It provides fast-response, chemically specific, high precision, and calibrated measurements of nitrogen oxides and ozone at a spatial resolution of better than 50m at typical WP-3D research flight speeds.

Detection is based on the gas-phase CL reaction of NO with O₃ at low pressure, resulting in photoemission from electronically excited NO₂. Photons are detected and quantified using pulse counting techniques, providing ~5 to 10 part-per-trillion by volume (pptv) precision at 1 Hz data rates.

One CL channel is used to measure ambient NO directly, a second channel is equipped with a high-power UV-LED converter to photodissociate ambient NO₂ to NO, and a third channel is equipped with a heated gold catalyst to reduce ambient NO_y species to NO. Reagent ozone is added to these sample streams to drive the CL reactions with NO. Ambient O₃ is detected in the fourth channel by adding reagent NO.

Instrument performance is routinely evaluated in flight by standard addition calibrations delivered within a few centimeters of the inlet tips. The separate NO and NO₂ sample paths, detectors, and inlet residence times are identical, permitting artifact-free calculation of ambient NO₂ by difference at high time resolution, with no lagging or smoothing relative to NO or to other fast-response measurements aboard the aircraft. A high-power UV-LED converter developed in our laboratory provides NO₂ conversion fractions exceeding 0.6 at a converter sample residence time of 0.11 seconds. This offers a significant advantage in terms of NO and NO₂ spatial resolution compared to other airborne NO₂ instruments. The NO_y channel is calibrated to NO, NO₂, and HNO₃ in flight and the O₃ channel is calibrated over an atmospherically relevant range of ozone mixing ratios in flight.

9. Proton transfer reaction mass spectrometer (PTR-MS): PI Martin

Graus, Carsten Warneke

Proton-transfer-reaction mass spectrometry (PTR-MS) (de Gouw et al., 2003; de Gouw and Warneke, 2007; Warneke et al., 2011) allows real-time measurements of volatile organic compounds (VOCs) in air with a high sensitivity and a fast time

response. In PTR-MS, proton-transfer reactions with H_3O^+ ions are used to ionize VOCs in air:

$$\text{H}_3\text{O}^+ + \text{VOC} \rightarrow \text{VOC.H}^+ + \text{H}_2\text{O}.$$

The air to be analyzed is continuously pumped through a drift tube reactor, where the VOCs are ionized in the proton-transfer reactions with H_3O^+ , produced in the hollow-cathode discharge ion source (Figure S4). H_3O^+ and product ions are detected with a quadrupole mass spectrometer. The inlet, shown in Figure S4, is pressure and temperature controlled and consists of PEEK and Teflon tubing and valves. Diverting the air through a catalytic converter that burns the VOCs periodically zeros the instrument. In between flights, sensitivity calibrations are performed using dynamically diluted VOC standards.

VOCs with a higher proton affinity than water can be detected by PTR-MS and usually reported are: methanol, acetonitrile, acetaldehyde, acetone, isoprene, sum of methyl vinyl ketone and methacrolein, methyl ethyl ketone, benzene, toluene, sum of C8-aromatics, sum of C9-aromatics, and sum of monoterpenes.

The PTR-MS has a response time of about 1 second and all compounds are measured for 1 second every 17 seconds at detection limits of 30-200 pptv and an uncertainty of 20-30% dependent on the VOC. The PTR-MS was set-up for SENEX nearly identical to what was used in many previous NOAA airborne field campaigns such as Calnex 2010 and ARCPAC 2008.

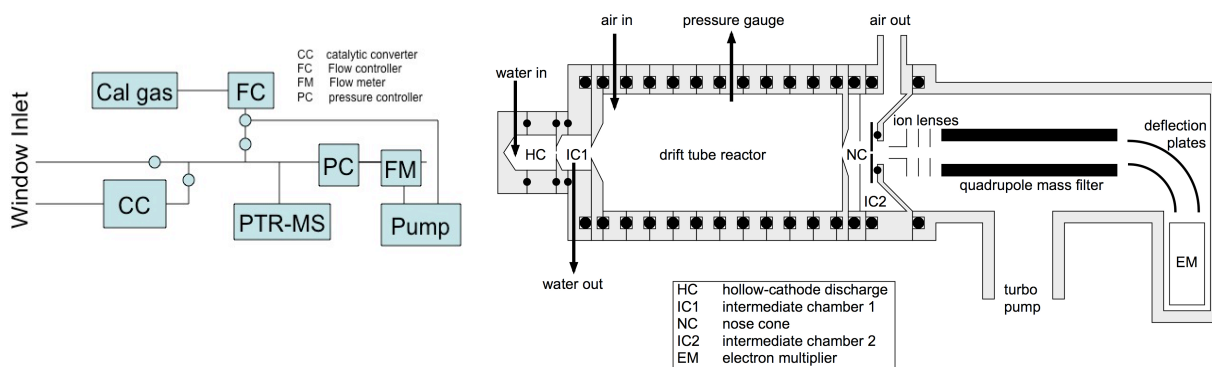


Figure S4: Schematic drawing of the PTR-MS instrument and the inlet.

10. Whole air sampler with immediate GC-MS analysis (iWAS/GCMS): PI

Jessica Gilman, Brian Lerner

The iWAS/GCMS is designed to speciate and quantify a variety of VOCs including alkanes, alkenes, biogenic VOCs (BVOCs), oxygenated VOCs (OVOCs), VOCs containing nitrogen, and halogenated VOCs in discrete air samples. iWAS/GCMS consists of 3 independent components: (1) onboard in-situ sample collection via 72 whole air sample (WAS) canisters, consistent of six 12-canister modules, located in AMPS pod on WP-3D, (2) in-field analysis of WAS canisters via gas chromatography-mass spectrometry (GC-MS), and (3) cleaning and conditioning of canisters for re-use on subsequent research flights. The canister design, collection, and conditioning protocols have been adopted from the NCAR AWAS system (Schauffler et al., 2003).

A detailed description of iWAS/GC-MS will be presented by Lerner et al. (2015). The onboard sampling system consists of a 316 SS forward-facing inlet, a stainless steel bellows compressor (Senior Aerospace), a sampling manifold, and 72 electro-polished stainless steel canisters (1.4 L). Each canister is isolated from the sample manifold by a stainless steel bellows valve actuated by a computer-controlled pneumatic valve system. The canisters may be automatically filled at regular time intervals during aerial surveys or triggered manually for targeted plume analysis. During sample collection, each canister is pressurized to approximately 50 psia by the compressor. Total sample acquisition time is typically 3-10 seconds depending upon ambient air pressure, which varies with aircraft altitude.

Post-flight, the canister modules are removed from the AMPS pod and connected to the analysis system via 1/8" silanized stainless steel tubing. The sample manifold is pumped out for approximately 2 hours to remove any residual water, then flushed with UHP nitrogen and evacuated before an individual canister is opened for analysis. This sequence of flushing and pumping is repeated before each canister is sampled.

Each canister is analyzed via gas chromatography-mass spectrometry (GC-MS). The custom-built GC-MS consists of two channels optimized for "light VOCs" (channel 1, C2-C6 compounds) and "heavier VOCs" (channel 2, C5-C11 compounds). Two 240 sccm samples are simultaneously collected from each canister. Prior to sample trapping, H₂O is removed from the sample stream via a cold trap (nominally

-45 and -35°C, respectively), and CO₂ is removed from the channel 1 sample via an ascarite scrubber. VOCs are pre-concentrated via cryogenic trapping at temperatures of -165 and -145°C for channels 1 and 2, respectively. The samples are analyzed sequentially with a porous layer open tubular (PLOT) Al₂O₃ column and a mid-polarity polysiloxane column for channels 1 and 2, respectively, with the analyte from both columns sent to a single quadrupole mass spectrometer detector run in selective ion mode for increased signal-to-noise. The entire sample pre-concentration (4 min) and separation/analysis/flush (16 min) is automatically repeated for subsequent canisters. All 72 canisters collected per flight were analyzed on-site between 12-100 hours after the aircraft had landed.

The GC-MS provides chemically detailed and highly sensitive measurements with detection limits in the 2-10 pptv range depending on the VOC. Each VOC is identified by its chromatographic retention time and electron-impact mass fragmentation pattern. All VOCs are individually calibrated using commercial and custom-made calibration standards. For SENEX, approximately 20 VOCs were quantified for each canister sample. A detailed description of the iWAS2 will be presented by Lerner et al. (2015).

After the canisters are analyzed, they are prepared and conditioned for reuse. Each canister is evacuated (<10 mTorr) and checked for leaks. The canisters are then heated to 75°C under vacuum, then filled with high purity nitrogen and re-evacuated. The nitrogen flush process is repeated a minimum of 3 times. Humidified nitrogen is added during the final flushing process in order to passivate the interior surfaces of the canisters.

11. Nitric Acid (HNO₃), Formic Acid (HCOOH) and HONO: PI Andy Neuman

HNO₃, HCOOH, and HONO were measured by chemical ionization mass spectrometry (CIMS) using I⁻ as a reagent ion (Neuman, 2015). The instrument included a heated inlet to deliver ambient air to the instrument, a flow tube where ions and ambient air reacted, and a quadrupole mass spectrometer for ion detection.

The 70-cm long inlet was housed in an aerodynamic winglet that was perpendicular to the aircraft fuselage. The inlet was temperature controlled to 40 C, and the total airflow through the inlet was 8 slm (Neuman et al., 2002). An all-Teflon valve located at the inlet tip was used to determine the instrument background signal. Every 30 minutes, the valve was actuated so that air was sampled for 1.5 min through a charcoal filter that removed HNO₃, HCOOH, and HONO from the air stream. The signal during these background measurements came from the instrument and was subtracted from the total signal to determine ambient mixing ratios. The inlet also included a port at the tip where calibration gas was added. HNO₃ and HCOOH at ppbv-levels were added to the inlet tip in-flight for 2 min approximately every hour. The HNO₃ and HCOOH sources were calibrated using permeation tubes. After each flight, the permeation tubes were removed from the aircraft and kept under constant flow and temperature, and the output from the HNO₃ calibration source was measured by UV optical absorption (Neuman et al., 2003). Mixing ratios were determined from these standard addition calibrations. The instrument was calibrated to HONO in the laboratory prior to the study, using HONO produced from the reaction of HCl with humidified NaNO₃ (Roberts et al., 2010).

Ambient air from the inlet was mixed with ions in a reduced pressure flow tube. Approximately 1.6 slm of the total 8 slm inlet flow was admitted through an orifice into a flow tube at 20 Torr and 20 C. The reagent ions were made in flight by flowing 2 slm N₂ doped with methyl iodide through a radioactive ²¹⁰Po ion source. This ions and ambient air reacted for approximately 200 ms in the flow tube. Since HNO₃ and HCOOH are more sensitive to water clustered with I-, water was added to the flow tube to prevent large changes in sensitivity with ambient water (Neuman et al., 2010; Zheng et al., 2011).

The quadrupole mass spectrometer was programmed to integrate signals from each of the product and reagent ions for a fraction of a second, in a sequence that repeated every second. As a result, an independent measurement for each compound was obtained once per second. Several times per flight the mass spectrometer was programmed to scan over the entire mass range (10 to 250 amu)

as a diagnostic of the ion chemistry stability. During instrument calibrations, zeroes, and mass scans, ambient measurements were not reported.

Measurement accuracy was determined from the variability of the instrument response to in-flight calibrations and from the uncertainty in the emission from the calibration sources. HNO_3 was measured with 25 pptv precision (for 1 s data) and an accuracy of $\pm(20\% + 50 \text{ pptv})$. HCOOH was measured with 40 pptv precision (for 1 s data) and an accuracy of $\pm(20\% + 120 \text{ pptv})$. HONO was measured with 25 pptv precision (for 1 s data) and an accuracy of $\pm(40\% + 30 \text{ pptv})$. The two accuracy terms represent uncertainties in the in-flight calibrations (%) and instrumental background measurements (pptv).

12. Ammonia (NH_3): PI John Nowak

Gas-phase NH_3 was measured during SENEX with a CIMS utilizing protonated acetone dimer $((\text{C}_3\text{H}_6\text{O})\text{H}^+(\text{C}_3\text{H}_6\text{O}))$ ion chemistry as described by Nowak et al (2007). Previously, this instrument was successfully deployed aboard the WP-3D during the 2004 New England Air Quality Study (NEAQS) (Nowak et al., 2007), the 2006 Texas Air Quality Study (TexAQS 2006) (Nowak et al., 2010), and the 2010 CalNex study (Nowak et al., 2012). The inlet, low-pressure flow tube reactor, and quadrupole mass spectrometer are similar to the airborne HNO_3 -CIMS described above.

In-flight standard addition calibrations and measurements of instrumental background signals were routinely performed to determine the sensitivity, stability, and time response of the instrument. Standard addition calibrations with 13 ppb of NH_3 were performed 3-5 times a flight with the output of a thermostated, flow-controlled, pressurized NH_3 permeation device (Kin-tek, La Marque, TX). The stability of the permeation device output was maintained between flights by removing the permeation oven from the aircraft and connecting it to a ground support system where the same flow and temperature conditions were maintained. The output of the NH_3 permeation device was quantified by UV absorption at 184.95 nm on the ground between each flight (Neuman et al., 2003) and varied less than 10% over the duration of the study. In-flight instrument sensitivity to NH_3 was 1 ion

counts/s/ppt (Hz/ppt) for 1×10^6 Hz of reagent ion signal as determined by the flow conditions.

The instrument background was determined in-flight by periodically pulling ambient air through a scrubber filled with commercially available silicon phosphates (Perma Pure, Inc). For most flights, the absolute background level ranged from 0.1 to 0.4 ppb. However, due to reduced flow conditions, on the June 11, 12, 16, and 18 flights, the observed absolute background levels were higher, ranging from 1.8 to 2.1 ppb. During most flights, the difference between consecutive backgrounds was 0.02 to 0.07 ppb. Again, for the flights of June 11, 12, 16, and 18, the difference between consecutive backgrounds was larger, ranging from 0.3 to 0.5 ppb. The instrument background signal is determined by interpolating between consecutive background measurements. Ambient mixing ratios were derived by subtracting the instrument background from the total signal. Typically, the overall 1σ uncertainty for the NH_3 measurement was estimated to be $\pm(25\% + 0.07 \text{ ppb}) + 0.02 \text{ ppbv}$ for a 1 s measurement with larger estimates for the June 11, 12, 16, and 18 flights.

The instrument time response to ambient variability was determined from the NH_3 signal decay following the removal of the calibration gas. These data were fitted with exponential decay curves, as described by Nowak et al (2007). On average the 2 e-folding signal decay time from a triple exponential fit ranged from 1 to 2 s with typically at least 80 % of the signal decay occurring within 1 s. Therefore, 1 s was used as the observed instrument time response during SENEX 2013 and in the data archive. 1 s instrument time response corresponds to a spatial resolution of ~ 100 m at typical WP-3D research flight speeds.

13. PAN: PI Jim Roberts, Patrick Veres

Acyl peroxy nitrates, (PANs), and nitryl chloride (ClNO_2) were measured onboard the WP-3D during SENEX using a thermal-decomposition chemical ionization mass spectrometer similar to the instrument originally described by Slusher et al (2004). The detection principle of PANs is thermal decomposition at 150°C followed by reaction of the resulting acyl peroxy radicals with iodide and

iodide water cluster ions ($I^- + I[H_2O]^-$) in an ion flow tube to produce a stable carboxylate $[RC(O)O^-]$ ion. The carboxylate ions are then measured with a quadrupole mass spectrometer. Nitryl chloride was detected as either ICl^- or $IClNO_2^-$ after reaction with $I^- + I[H_2O]^-$.

The instrument flow configuration used for PANs was based on that described by Slusher et al [2004] with some modifications. Ambient air was sampled from outside the aircraft through a 6.3 mm OD PFA tube, temperature controlled at 30°C, inside a small winglet that extended approximately 37cm from the skin of the aircraft. The airflow was then directed to the inlet system of the instrument through a 9mm OD PFA tube at cabin temperature. The inlet system consisted of a pair of PFA valves, configured such that the air flow can be periodically directed through a zeroing loop consisting of a 1.5m length of 6.3mm OD stainless steel tube held at 225°C, sufficient to thermally decompose essentially all the PAN compounds in the sample stream, and approximately 95% of $ClNO_2$. A small flow of ^{13}C -labeled PAN was added through a normally-open port of a 3-way valve (Zheng et al., 2011). The valve permitted the labeled standard to be switched out of line periodically to determine instrument backgrounds, and to check for cross-sensitivities at other masses due to proton transfer chemistry involving acetate ions (Veres et al., 2008). The airflow then passed through a pressure reduction pinhole into a heated zone consisting of 25cm long section of 9mm OD FEP tubing held at 150°C. The exit of this tube was connected to the ion flow tube via another stainless steel pinhole. The ion flow tube was operated at a pressure of 25 Torr, controlled by bleeding cabin air into the pump line with a pressure controller (MKS 640). Ions were introduced into the flow tube by passing 2 SLPM of 3ppmv methyl iodide through a ^{210}Po ionizer. A small flow of N_2 saturated with water was added to the front of the ion flow tube, in order to keep the flow tube humidity above the thresholds at which the ion chemistry is dominated by $I[H_2O]^-$ clusters (Kercher et al., 2009; Mielke et al., 2011; Slusher et al., 2004; Zheng et al., 2011).

The instrument was operated in selected ion mode switching among 10 ions in succession, every 2 seconds, dwelling on each one for 0.1sec in the case of I^- and

0.2 sec for the other 9. The inlet operation sequence provided a zero lasting 30 sec every 10 minutes. In addition, the labeled standard was turned off for 30 sec every 10 min, 5 minutes apart from the zeros.

On-line calibration of the instrument for PANs was accomplished through the constant addition of $^{13}\text{C}_2$ -labelled PAN that is produced in a pressure-controlled photosource similar to that described by Zheng et al (2011). PAN was produced with an efficiency of $93\pm 5\%$ from a nitric oxide standard as determined from measurements of NO_x and NO_y using the CRDS instrument. The other PAN compounds were calibrated relative to this photosource before and after the project with the methods described by Veres and Roberts (2015). Nitryl chloride was calibrated using a portable source that uses the reaction of molecular chlorine (Cl_2) with sodium nitrite (NaNO_2) as described by Thaler et al (2011) with the output of the source calibrated by thermal decomposition at 350°C and detection by NO_2 using CRDS as described by Wild et al (2014).

The propagated uncertainties in the ^{13}C PAN calibration, flows, and instrument zero determinations result in an overall accuracy for PAN measurements of $\pm(15\% + 5\text{pptv})$, and $\pm(20\% + 5\text{pptv})$ for the other PAN species. The uncertainty of ClNO_2 , measured at the ICl^- mass was $\pm(30\% + 25\text{pptv})$. Roiger et al (2011) have pointed out that the use of a ^{13}C PAN standard for measuring native PAN at mass 59 requires a correction for the natural abundance of heavy isotopes. Since the ^{13}C labeled acetone used for the photosource is rated at 99% purity per carbon, the corresponding correction for our PAN standard would be about 3% and we chose not to correct our ambient PAN for heavy isotopes. Phillips et al., [2012] have observed peroxyacetic acid conversion to acetate in their PAN CIMS. Several tests before and during SENEX were performed to explore whether our PAN CIMS had similar sensitivity. Cold inlet (i.e. no thermal decomposition), NO addition to titrate $\text{CH}_3\text{C}(\text{O})\text{OO}$ radicals and possible signal modulation at carboxylate masses when the ^{13}C PAN standard is switched out all indicated no significant signals due to peroxyacids.

14. Multifunctional Organic Molecules and Inorganics by I-CIMS:: PI Joel

A. Thornton, Felipe D. Lopez-Hilfiker, Ben H. Lee

The instrument used consisted of a reduced-pressure ion–molecule reaction (IMR) region, coupled to an atmospheric pressure interface HR-ToF-MS (Tofwerk AG, Thun, Switzerland) (Lee et al., 2014).

Ambient air is drawn through a critical orifice at 2.0 standard liters per minute (slpm) into the IMR, which is held at 90 mbar by means of a scroll pump (Agilent IDP3) and a custom servo-controlled vacuum valve used to continuously regulate pumping speed. The pressure varies by <1% even as ambient pressure changes by factors of 5. The IMR temperature is controlled to within 0.2 °C at a set point between ambient and 40 °C depending upon application. Up to two commercial radioactive ion sources (Po-210, 10 mCi, NRD) oriented 90° apart and orthogonal to the ion–molecule reaction mixture flow can be used for switching between positive and negative reagent ions. The IMR also contains a diffusion cell to continuously deliver calibration compounds for converting measured ion flight times into m/Q.

Iodide ions are generated by passing a 2 slpm flow of ultrahigh purity (UHP) N₂ over a permeation tube filled with methyl iodide and then through the Po-210 ion source into the IMR. The ionizer and sample flows mix and interact for ~120 ms until a fraction is sampled through an orifice into a 4-stage differentially pumped chamber housing the HR-ToF-MS. The first stage is held at 2 mbar by a molecular drag pump (Alcatel MDP 5011), and the second stage is held at 0.01 mbar by a split-flow turbo molecular pump (Pfeiffer). Two quadrupole ion guides transmit the ions through these two stages while providing collisional cooling and thus energetic homogenization of the ions as they enter the third “extractor” region. In the third and final stages, additional optics further focus the ions prior to being orthogonally pulsed at 22.22 kHz into the drift region where their arrival time after a V-mode trajectory is detected with a pair of microchannel plate detectors (Photonis Inc., U.S.A.).

Minimizing sampling losses of low volatility species is a priority. Ambient air is drawn at 22 slpm through a 72 cm long 1.6 cm inner diameter

polytetrafluoroethylene (PTFE) tubing by a dedicated scroll pump (Agilent IDP3). The first 25 cm of the inlet tube is housed in an aerodynamic winglet that extends outside of the boundary layer of the WP-3D aircraft. We estimate an inlet residence time of approximately 0.4 s at 1013 hPa while maintaining laminar flow ($Re \sim 1900$). A small fraction of the centerline flow (2 slpm) is sampled through a conical-shaped critical orifice into the IMR, while the remainder is exhausted through four radially symmetric ports located downstream and around the raised sampling orifice. The inlet is heated to 40 °C to minimize condensation on the tubing surface and to maintain a constant sampling environment under rapidly evolving outside and cabin conditions.

The instrument background signal is established by introducing dry UHP N₂ directly in front of the critical orifice every 15 minutes to displace the incoming ambient air during flight. This addition is achieved by a servo-controlled, 7 cm (2.8 in.) long 0.3 cm (1/8 in.) diameter stainless steel probe that when actuated, enters from the side of the inlet at a 45° angle and is positioned directly upstream of, but not in contact with, the sampling cone. Ambient air is rejected from the IMR by overblowing the sampling orifice with N₂ (~3 slpm). When not in use, the probe is retracted so that it resides outside of the sample streamline. Instrument sensitivity dependence on water vapor pressure is accounted for, but given that the sensitivity for most organic compounds is higher in dry air, the measured background is more than likely an upper limit.

The stability of the instrument is determined by continuously delivering ¹³C-labeled formic acid, ¹³CH₂O₂, through a 30 gauge 1.5 cm long needle bored through the PTFE inlet near the inlet entrance. The ¹³CH₂O₂ (Cambridge Isotopes) was contained in a custom-built PTFE permeation tube, held at constant temperature (40 °C) and pressure. The permeation rate was determined gravimetrically and compared to independently verified ¹²CH₂O₂ permeation tubes (KIN-TEK). Any drift in the instrument sensitivity measured by the I(¹³CH₂O₂)⁻ ion signal, not due to ambient water vapor, is similarly applied to all other species using relative sensitivities which have been determined in the laboratory.

15. Cavity enhanced absorption spectroscopy for glyoxal (ACES): PI

Kyung-Eun Min, Rebecca Washenfelder, Steve Brown

Glyoxal is one of the key reactive intermediates in the atmospheric oxidation of hydrocarbons, particularly biogenic VOCs and aromatic compounds (Fu et al., 2008). It is the simplest α -dicarbonyl species, and it can serve either as a source of radicals through its photolysis or as a source of secondary organic aerosol through its heterogeneous uptake and subsequent oligomerization. It also has strong visible absorption bands that facilitate its detection via spectroscopic methods. Cavity enhanced spectroscopy, CES, is a recently developed technique for high-sensitivity, spectrally resolved measurements (Fiedler et al., 2003). As shown in Figure S5, it employs a broadband light source, such as a light emitting diode (LED), an optical cavity and a grating spectrometer. The technique can achieve optical path lengths of several tens of kilometers for measurements of atmospheric trace gases at sub part per billion levels.

The CES technique has been demonstrated for measurement of glyoxal in both the laboratory (Washenfelder et al., 2008) and in the field during CalNex 2010 (Washenfelder et al., 2011b; Young et al., 2012). Ground based CES measurements during the CalNex 2010 campaign also included NO_2 and HONO (Young et al., 2012).

For SENEX, a new aircraft version of the instrument achieved robust performance using a custom optical mounting system, high power LEDs with electronic on/off modulation, state-of-the-art cavity mirrors, and materials that minimize analyte surface losses (Min et al., 2015). The aircraft instrument is called the Airborne Cavity Enhanced Spectrometer (ACES). The ACES instrument has two channels with wavelength coverage from 361–389 nm and 438–468 nm. The wavelength range is determined by the LED spectral radiance, the center wavelength and bandwidth of the cavity mirrors, as well as the wavelength-dependent absorption features of target gases. HONO and NO_2 are detected at 361–389 nm, while CHOCHO, CH_3COCHO , NO_2 , and H_2O are detected at 438–468 nm. The demonstrated precision (2σ) for retrievals of CHOCHO, HONO and NO_2 are 34, 350 and 80 pptv in 5 s (Min et al., 2015). The accuracy is 5.8%, 9.0% and 5.0%, limited mainly by the available absorption cross section (Min et al., 2015).

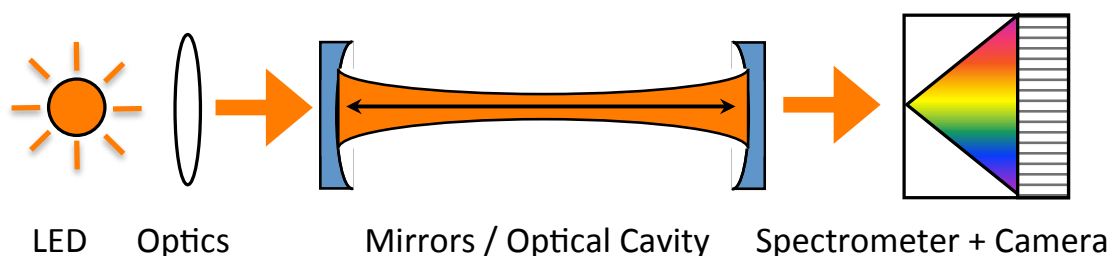


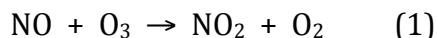
Figure S5. Simplified schematic of the broadband CES instrument

16. Cavity Ring Down Spectroscopy (CRDS): PI Peter Edwards, Steve Brown

Cavity ring-down spectroscopy (CRDS) is a high sensitivity optical technique for the measurement of trace gas concentration applicable to nitrogen oxides. The NOAA CRDS instrument for nitrogen oxides and ozone is based on two visible diode lasers at 662 nm (for detection of NO_3) and 405 nm (for detection of NO_2) (Wagner et al., 2011). Inlet conversions allow the measurement of additional species. Figure S6 shows a schematic of the instrument.

One 662 nm channel provides a direct measurement of NO_3 , while a second 662 nm channel with a heated inlet provides a measurement of the sum of NO_3 and N_2O_5 via thermal dissociation of N_2O_5 to NO_3 . Both channels are zeroed by addition of NO to the inlet, which reacts rapidly with NO_3 , but not with other species that absorb 662 nm light, such as ambient NO_2 , O_3 or water vapor (Dubé et al., 2006). The NO_2 produced in this reaction has an absorption cross section nearly 10^4 times smaller than NO_3 and therefore does not interfere with the NO_3 measurement.

There are three channels at 405 nm. The first detects NO_2 directly by total optical extinction at this wavelength, which is specific to NO_2 . The second channel has an addition of excess O_3 to convert NO to NO_2 to measure total NO_x ($=\text{NO} + \text{NO}_2$) via reaction (1) (Fuchs et al., 2009).



A third 405 nm channel has an addition of excess NO to quantitatively convert O_3 to NO_2 to measure total O_x ($=\text{O}_3 + \text{NO}_2$), also via reaction (2)

(Washenfeller et al., 2011a). Differencing between the NO_x , O_x channels and the NO_2 channel provides measurement of NO and O_3 , respectively. The zero for the 405 nm channel consists of addition of clean air to the inlet. All channels operate at a repetition rate of 4 Hz. During SENEX, the 1 Hz measurement precision (2σ) was 3 pptv for NO_3 and N_2O_5 , measurement precision for NO_2 and O_3 was <50 pptv, but the uncertainty in the zero for these species was 200 pptv due to an uncertainty in the relative humidity of the scrubbed air used for zeroing the instrument. The precision of the NO measurement was significantly degraded during SENEX due to a mechanical instability in the optical alignment of this cavity. This compound was not reported for the majority of flights, but had a precision of 1 ppbv for the small number of flights with large power plant plume intercepts containing measurable NO .

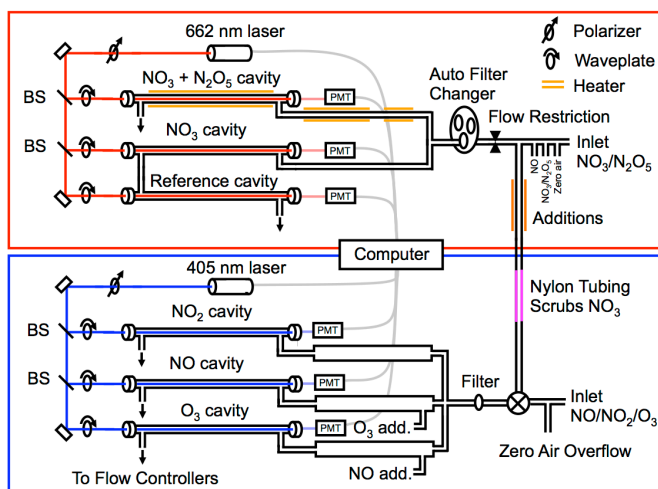


Figure S6. Schematics of the nitrogen oxide CRDS instrument.

17. In situ Airborne Formaldehyde (ISAF): PI Frank Keutsch, Thomas Hanisco, Glenn Wolfe

The NASA GSFC In Situ Airborne Formaldehyde (ISAF) instrument uses laser induced fluorescence (LIF) to provide fast, sensitive observations of formaldehyde (HCHO) throughout the troposphere and lower stratosphere (Cazorla et al., 2015). A particle-rejecting inlet draws sample air into the low-pressure detection region at ~ 3 standard liters per minute. A pulsed tunable fiber laser (NovaWave TFL) excites

a single rotational transition of the A – X band at 353.16 nm, and the resulting fluorescence is detected with a photon counting photo multiplier tube. Dithering the laser on and off resonance with the rotational feature provides a continuous measure of spectroscopic background and greatly reduces the potential for measurement artifacts. The difference between power-normalized on- and off-resonance signals is proportional to the mixing ratio of HCHO. Laser wavelength is monitored via a separate reference cell containing a high concentration of HCHO.

The sensitivity of the LIF technique is dependent on laser power and the pressure in the detection cell. At 10 mW and 100 mbar, the detection limit is ~36 pptv for 1 s integration and S/N = 2. The nominal sampling frequency is 10 Hz, and mixing ratios are typically reported at 1 Hz. The instrument was calibrated pre- and post-mission with standard addition of formaldehyde gas mixtures. The 1- σ accuracy of the measurement is $\pm 10\%$.

References:

Allan, J. D., Delia, A. E., Coe, H., Bower, K. N., Alfarra, M. R., Jimenez, J. L., Middlebrook, A. M., Drewnick, F., Onasch, T. B., Canagaratna, M. R., Jayne, J. T., and Worsnop, D. R.: A generalised method for the extraction of chemically resolved mass spectra from Aerodyne aerosol mass spectrometer data, *J. Aerosol Sci.*, 35, 909-922, 2004.

Allan, J. D., Jimenez, J. L., Williams, P. I., Alfarra, M. R., Bower, K. N., Jayne, J. T., Coe, H., and Worsnop, D. R.: Quantitative sampling using an Aerodyne aerosol mass spectrometer 1. Techniques of data interpretation and error analysis, *J. Geophys. Res.*, 108, 4090, 2003.

Bahreini, R., Dunlea, E. J., Matthew, B. M., Simons, C., Docherty, K. S., DeCarlo, P. F., Jimenez, J. L., Brock, C. A., and Middlebrook, A. M.: Design and operation of a pressure-controlled inlet for airborne sampling with an aerodynamic aerosol lens, *Aerosol Sci. Technol.*, 42, 465-471, 2008.

Bahreini, R., Ervens, B., Middlebrook, A. M., Warneke, C., de Gouw, J. A., DeCarlo, P. F., Jimenez, J. L., Brock, C. A., Neuman, J. A., Ryerson, T. B., Stark, H., Atlas, E., Brioude, J., Fried, A., Holloway, J. S., Peischl, J., Richter, D., Walega, J., Weibring, P., Wollny, A. G., and Fehsenfeld, F. C.: Organic aerosol formation in urban and industrial plumes near Houston and Dallas, Texas, *J. Geophys. Res.*, 114, D00F16, 2009.

Brock, C. A., Cozic, J., Bahreini, R., Froyd, K. D., Middlebrook, A. M., McComiskey, A., Brioude, J., Cooper, O. R., Stohl, A., Aikin, K. C., de Gouw, J. A., Fahey, D. W., Ferrare, R. A., Gao, R. S., Gore, W., Holloway, J. S., Hubler, G., Jefferson, A., Lack, D. A., Lance, S., Moore, R. H., Murphy, D. M., Nenes, A., Novelli, P. C., Nowak, J. B., Ogren, J. A., Peischl, J., Pierce, R. B., Pilewskie, P., Quinn, P. K., Ryerson, T. B., Schmidt, K. S., Schwarz, J. P., Sodemann, H., Spackman, J. R., Stark, H., Thomson, D. S., Thornberry, T., Veres, P., Watts, L. A., Warneke, C., and Wollny, A. G.: Characteristics, sources, and transport of aerosols measured in spring 2008 during the aerosol, radiation, and cloud processes affecting Arctic Climate (ARCPAC) Project, *Atmos. Chem. Phys.*, 11, 2423-2453, 2011.

Brock, C. A., Schroder, F., Bernd, K., Petzold, A., Busen, R., and Fiebig, M.: Ultrafine particle size distributions measured in aircraft exhaust plumes, *J. Geophys. Res.*, 105, 26,555-526,567, 2000.

Canagaratna, M. R., Jayne, J. T., Jimenez, J. L., Allan, J. D., Alfarra, M. R., Zhang, Q., Onasch, T. B., Drewnick, F., Coe, H., Middlebrook, A., Delia, A., Williams, L. R., Trimborn, A. M., Northway, M. J., DeCarlo, P. F., Kolb, C. E., Davidovits, P., and Worsnop, D. R.: Chemical and microphysical characterization of ambient aerosols

with the Aerodyne aerosol mass spectrometer, *Mass Spectrom. Rev.*, 26, 185-222, 2007.

Cazorla, M., Wolfe, G. M., Bailey, S. A., Swanson, A. K., Arkinson, H. L., and Hanisco, T. F.: A new airborne laser-induced fluorescence instrument for in situ detection of formaldehyde throughout the troposphere and lower stratosphere, *Atmospheric Measurement Techniques*, 8, 541-552, 2015.

Cross, E. S., Onasch, T. B., Canagaratna, M., Jayne, J. T., Kimmel, J., Yu, X.-Y., Alexander, M. L., Worsnop, D. R., and Davidovits, P.: Single particle characterization using a light scattering module coupled to a time-of-flight aerosol mass spectrometer., *Atmos. Chem. Phys.*, 9, 7769-7793, 2009.

Cross, E. S., Slowik, J. G., Davidovits, P., Allan, J. D., Worsnop, D. R., Jayne, J. T., Lewis, D. K., Canagaratna, M., and Onasch, T. B.: Laboratory and ambient particle density determinations using light scattering in conjunction with aerosol mass spectrometry, *Aerosol Sci. Technol.*, 41, 343-359, 2007.

de Gouw, J., Warneke, C., Karl, T., Eerdekens, G., van der Veen, C., and Fall, R.: Sensitivity and specificity of atmospheric trace gas detection by proton-transfer-reaction mass spectrometry, *International Journal of Mass Spectrometry*, 223, 365-382, 2003.

de Gouw, J. A. and Warneke, C.: Measurements of volatile organic compounds in the earths atmosphere using proton-transfer-reaction mass spectrometry, *Mass Spectrometry Reviews*, 26, 223-257, 2007.

DeCarlo, P. F., Kimmel, J. R., Trimborn, A., Northway, M. J., Jayne, J. T., Aiken, A. C., Gonin, M., Fuhrer, K., Horvath, T., Docherty, K. S., Bates, D. R., and Jimenez, J. L.: Field-Deployable, High-Resolution, Time-of-Flight Aerosol Mass Spectrometer, *Anal. Chem.*, 78, 8281-8289, doi: 8210.1021/ac061249n, 2006.

Drewnick, F., Hings, S. S., DeCarlo, P., Jayne, J. T., Gonin, M., Fuhrer, K., Weimer, S., Jimenez, J. L., Demerjian, K. L., Borrmann, S., and Worsnop, D. R.: A new time-of-flight aerosol mass spectrometer (TOF-AMS) - Instrument description and first field deployment, *Aerosol Sci. Technol.*, 39, 637-658, 2005.

Dubé, W. P., Brown, S. S., Osthoff, H. D., Nunley, M. R., Ciciora, S. J., Paris, M. W., McLaughlin, R. J., and Ravishankara, A. R.: Aircraft instrument for simultaneous, in-situ measurements of NO₃ and N₂O₅ via cavity ring-down spectroscopy, *Rev. Sci. Instr.*, 77, 034101, 2006.

Fiedler, S. E., Hese, A., and Ruth, A. A.: Incoherent broad-band cavity-enhanced absorption spectroscopy, *Chemical Physics Letters*, 371, 284-294, 2003.

Fu, T.-M., Jacob, D. J., Wittrock, F., Burrows, J. P., Vrekoussis, M., and Henze, D. K.: Global budgets of atmospheric glyoxal and methylglyoxal, and implications for formation of secondary organic aerosols, *J. Geophys. Res.-Atmos.*, 113, 2008.

Fuchs, H., Dubé, W. P., Lerner, B. M., Wagner, N. L., Williams, E. J., and Brown, S. S.: A sensitive and versatile detector for atmospheric NO₂ and NO_x based on blue diode laser cavity ring-down spectroscopy, *Environ. Sci. Technol.*, 43, 7831-7836, 2009.

Holloway, J. S., Jakoubek, R. O., Parrish, D. D., Gerbig, C., Volz-Thomas, A., Schmitgen, S., Fried, A., Wert, B., Henry, B., and Drummond, J. R.: Airborne intercomparison of vacuum ultraviolet fluorescence and tunable diode laser absorption measurements of tropospheric carbon monoxide, *J. Geophys. Res.*, 105, 24,251-224,261, 2000.

Jayne, J. T., Leard, D. C., Zhang, X., Davidovits, P., Smith, K. A., Kolb, C. E., and Worsnop, D. R.: Development of an aerosol mass spectrometer for size and composition analysis of submicron particles, *Aerosol Sci. Technol.*, 33, 49-70, 2000.

Jimenez, J. L., Jayne, J. T., Shi, Q., Kolb, C. E., Worsnop, D. R., Yourshaw, I., Seinfeld, J. H., Flagan, R. C., Zhang, X., Smith, K. A., Morris, J. W., and Davidovits, P.: Ambient aerosol sampling using the Aerodyne aerosol mass spectrometer, *J. Geophys. Res.*, 108, 8425, 2003.

Kercher, J. P., Riedel, T. P., and Thornton, J. A.: Chlorine activation by N₂O₅: simultaneous, in situ detection of ClNO₂ and N₂O₅ by chemical ionization mass spectrometry, *Atmospheric Measurement Techniques*, 2, 193-204, 2009.

Kondo, Y., Matsui, H., Moteki, N., Sahu, L., Takegawa, N., Kajino, M., Zhao, Y., Cubison, M. J., Jimenez, J. L., Vay, S., Diskin, G. S., Anderson, B., Wisthaler, A., Mikoviny, T., Fuelberg, H. E., Blake, D. R., Huey, G., Weinheimer, A. J., Knapp, D. J., and Brune, W. H.: Emissions of black carbon, organic, and inorganic aerosols from biomass burning in North America and Asia in 2008, *J. Geophys. Res.-Atmos.*, 116, 2011.

Lack, D. A., Richardson, M. S., Law, D., Langridge, J. M., Cappa, C. D., McLaughlin, R. J., and Murphy, D. M.: Aircraft Instrument for Comprehensive Characterization of Aerosol Optical Properties, Part 2: Black and Brown Carbon Absorption and Absorption Enhancement Measured with Photo Acoustic Spectroscopy, *Aerosol Science and Technology*, 46, 555-568, 2012.

Lance, S., Medina, J., Smith, J. N., and Nenes, A.: Mapping the operation of the DMT Continuous Flow CCN counter, *Aerosol Science and Technology*, 40, 242-254, 2006.

Langridge, J. M., Richardson, M. S., Lack, D., Law, D., and Murphy, D. M.: Aircraft Instrument for Comprehensive Characterization of Aerosol Optical Properties, Part I: Wavelength-Dependent Optical Extinction and Its Relative

Humidity Dependence Measured Using Cavity Ringdown Spectroscopy, *Aerosol Science and Technology*, 45, 1305-1318, 2011.

Lee, B. H., Lopez-Hilfiker, F. D., Mohr, C., Kurten, T., Worsnop, D. R., and Thornton, J. A.: An Iodide-Adduct High-Resolution Time-of-Flight Chemical-Ionization Mass Spectrometer: Application to Atmospheric Inorganic and Organic Compounds, *Environ. Sci. Technol.*, 48, 6309-6317, 2014.

Lerner, B., Gilman, J. B., Dumas, M., Hughes, D. D., Jaksich, A., Hatch, C. D., Graus, M., Tokarek, T. W., Peischl, J., Koss, A., Yuan, B., Warneke, C., Isaacman-Van Wertz, G., Sueper, D., and de Gouw, J. A.: An improved, automated whole-air sampler and VOC GC-MS analysis system, *Atmospheric measurement Techniques Discussions*, in preparation, 2015.

Liu, P., Ziemann, P. J., Kittelson, D. B., and McMurry, P. H.: Generating Particle Beams of Controlled Dimensions and Divergence: I. Theory of Particle Motion in Aerodynamic Lenses and Nozzle Expansion, *Aerosol Sci. Technol.*, 22, 293-313, 1995.

Liu, S., Russell, L. M., Sueper, D. T., and Onasch, T. B.: Organic particle types by single-particle measurements using a time-of-flight aerosol mass spectrometer coupled with a light scattering module, *Atmos. Meas. Tech. Discuss.*, 5, 3047-3077, 2012.

Matthew, B. M., Middlebrook, A. M., and Onasch, T. B.: Collection efficiencies in an Aerodyne aerosol mass spectrometer as a function of particle phase for laboratory generated aerosols, *Aerosol Sci. Technol.*, 42, 884-898, 2008.

Middlebrook, A. M., Bahreini, R., Jimenez, J. L., and Canagaratna, M. R.: Evaluation of composition-dependent collection efficiencies for the Aerodyne aerosol mass spectrometer using field data, *Aerosol Sci. Technol.*, 46, 258-271, 2012.

Mielke, L. H., Furgeson, A., and Osthoff, H. D.: Observation of ClNO₂ in a Mid-Continental Urban Environment, *Environ. Sci. Technol.*, 45, 8889-8896, 2011.

Min, K. E., Washenfelder, R. A., Dube, W. P., Langford, A. O., Edwards, P. M., Zarzana, K. J., Stutz, J., Lu, K., Zhang, Y., and Brown, S. S.: A broadband cavity enhanced absorption spectrometer for aircraft measurements of glyoxal, methyl glyoxal, nitrous acid, nitrogen dioxide, and water vapor, *Atmospheric measurement Techniques Discussions*, submitted, 2015.

Moore, R. H., Cerully, K., Bahreini, R., Brock, C. A., Middlebrook, A. M., and Nenes, A.: Hygroscopicity and composition of California CCN during summer 2010, *J. Geophys. Res.-Atmos.*, 117, 2012.

Moore, R. H. and Nenes, A.: Scanning Flow CCN Analysis-A Method for Fast Measurements of CCN Spectra, *Aerosol Science and Technology*, 43, 1192-1207, 2009.

Neuman, J. A.: HONO sources to the troposphere in the Southeast U.S., in preparation, 2015. 2015.

Neuman, J. A., Huey, L. G., Dissly, R. W., Fehsenfeld, F. C., Flocke, F., Holecek, J. C., Holloway, J. S., Hubler, G., Jakoubek, R., Nicks Jr., D. K., Parrish, D. D., Ryerson, T. B., Sueper, D. T., and Weinheimer, A. J.: Fast-response airborne in situ measurements of HNO₃ during the Texas 2000 Air Quality Study, *J. Geophys. Res.*, 107, 4436, doi:4410.1029/2001JD001437, 2002.

Neuman, J. A., Nowak, J. B., Huey, L. G., Burkholder, J. B., Dibb, J. E., Holloway, J. S., Liao, J., Peischl, J., Roberts, J. M., Ryerson, T. B., Scheuer, E., Stark, H., Stickel, R. E., Tanner, D. J., and Weinheimer, A.: Bromine measurements in ozone depleted air over the Arctic Ocean, *Atmos. Chem. Phys.*, 10, 6503-6514, 2010.

Neuman, J. A., Ryerson, T. B., Huey, L. G., Jakoubek, R., Nowak, J. B., Simons, C., and Fehsenfeld, F. C.: Calibration and evaluation of nitric acid and ammonia permeation tubes by UV optical absorption, *Environ. Sci. Technol.*, 37, 2975-2981, 2003.

Nowak, J. B., Neuman, J. A., Bahreini, R., Brock, C. A., Middlebrook, A. M., Wollny, A. G., Holloway, J. S., Peischl, J., Ryerson, T. B., and Fehsenfeld, F. C.: Airborne observations of ammonia and ammonium nitrate formation over Houston, Texas, *J. Geophys. Res.-Atmos.*, 115, 2010.

Nowak, J. B., Neuman, J. A., Bahreini, R., Middlebrook, A. M., Holloway, J. S., McKeen, S. A., Parrish, D. D., Ryerson, T. B., and Trainer, M.: Ammonia sources in the California South Coast Air Basin and their impact on ammonium nitrate formation, *Geophys. Res. Lett.*, 39, 2012.

Nowak, J. B., Neuman, J. A., Kozai, K., Huey, L. G., Tanner, D. J., Holloway, J. S., Ryerson, T. B., Frost, G. J., McKeen, S. A., and Fehsenfeld, F. C.: A chemical ionization mass spectrometry technique for airborne measurements of ammonia, *J. Geophys. Res.-Atmos.*, 112, 2007.

Peischl, J., Ryerson, T. B., Holloway, J. S., Trainer, M., Andrews, A. E., Atlas, E. L., Blake, D. R., Daube, B. C., Dlugokencky, E. J., Fischer, M. L., Goldstein, A. H., Guha, A., Karl, T., Kofler, J., Kosciuch, E., Misztal, P. K., Perring, A. E., Pollack, I. B., Santoni, G. W., Schwarz, J. P., Spackman, J. R., Wofsy, S. C., and Parrish, D. D.: Airborne observations of methane emissions from rice cultivation in the Sacramento Valley of California, *J. Geophys. Res.-Atmos.*, 117, 2012.

Pollack, I. B., Lerner, B. M., and Ryerson, T. B.: Evaluation of ultraviolet light-emitting diodes for detection of atmospheric NO₂ by photolysis - chemiluminescence, *Journal of Atmospheric Chemistry*, 65, 111-125, 2010.

Raatikainen, T., Moore, R. H., Lathem, T. L., and Nenes, A.: A coupled observation - modeling approach for studying activation kinetics from measurements of CCN activity, *Atmos. Chem. Phys.*, 12, 4227-4243, 2012.

Roberts, G. C. and Nenes, A.: A continuous-flow streamwise thermal-gradient CCN chamber for atmospheric measurements, *Aerosol Science and Technology*, 39, 206-221, 2005.

Roberts, J. M., Veres, P., Warneke, C., Neuman, J. A., Washenfelder, R. A., Brown, S. S., Baasandorj, M., Burkholder, J. B., Burling, I. R., Johnson, T. J., Yokelson, R. J., and de Gouw, J.: Measurement of HONO, HNCO, and other inorganic acids by negative-ion proton-transfer chemical-ionization mass spectrometry (NI-PT-CIMS): application to biomass burning emissions, *Atmospheric Measurement Techniques*, 3, 981-990, 2010.

Roiger, A., Aufmhoff, H., Stock, P., Arnold, F., and Schlager, H.: An aircraft-borne chemical ionization - ion trap mass spectrometer (CI-ITMS) for fast PAN and PPN measurements, *Atmospheric Measurement Techniques*, 4, 173-188, 2011.

Ryerson, T. B., Buhr, M. P., Frost, G. J., Goldan, P. D., Holloway, J. S., Hübler, G., Jobson, B. T., Kuster, W. C., McKeen, S. A., Parrish, D. D., Roberts, J. M., Sueper, D. T., Trainer, M., Williams, J., and Fehsenfeld, F. C.: Emissions lifetimes and ozone formation in power plant plumes, *J. Geophys. Res.*, 103, 22,569-522,583, 1998.

Ryerson, T. B., Huey, L. G., Knapp, K., Neuman, J. A., Parrish, D. D., Sueper, D. T., and Fehsenfeld, F. C.: Design and initial characterization of an inlet for gas-phase NO_y measurements from aircraft, *J. Geophys. Res.*, 104, 5483-5492, 1999.

Ryerson, T. B., Williams, E. J., and Fehsenfeld, F. C.: An efficient photolysis system for fast-response NO₂ measurements, *J. Geophys. Res.*, 105, 26,447-426,461, 2000.

Schauffler, S. M., Atlas, E. L., Donnelly, S. G., Andrews, A., Montzka, S. A., Elkins, J. W., Hurst, D. F., Romashkin, P. A., Dutton, G. S., and Stroud, V.: Chlorine budget and partitioning during the Stratospheric Aerosol and Gas Experiment (SAGE) III Ozone Loss and Validation Experiment (SOLVE), *J. Geophys. Res.-Atmos.*, 108, 2003.

Schwarz, J. P., Spackman, J. R., Fahey, D. W., Gao, R. S., Lohmann, U., Stier, P., Watts, L. A., Thomson, D. S., Lack, D. A., Pfister, L., Mahoney, M. J., Baumgardner, D., Wilson, J. C., and Reeves, J. M.: Coatings and their enhancement of black carbon light absorption in the tropical atmosphere, *J. Geophys. Res.-Atmos.*, 113, 2008.

Schwarz, J. P., Spackman, J. R., Gao, R. S., Watts, L. A., Stier, P., Schulz, M., Davis, S. M., Wofsy, S. C., and Fahey, D. W.: Global-scale black carbon profiles observed in the remote atmosphere and compared to models (vol 37, art L18812 , 2010), *Geophys. Res. Lett.*, 37, 2010.

Slowik, J. G., Stroud, C., Bottenheim, J. W., Brickell, P. C., Chang, R. Y.-W., Liggiro, J., Makar, P. A., Martin, R. V., Moran, M. D., Shantz, N. C., Sjostedt, S. J., Donkelaar, A. v., Vlasenko, A., Wiebe, H. A., Xia, A. G., Zhang, J., Leaitch, W. R., and Abbatt, J. P. D.: Characterization of a large biogenic secondary organic aerosol event from eastern Canadian forests, *Atmos. Chem. Phys.*, 10, 2825-2845, 2010.

Slusher, D. L., Huey, L. G., Tanner, D. J., Flocke, F. M., and Roberts, J. M.: A thermal dissociation-chemical ionization mass spectrometry (TD-CIMS) technique for the simultaneous measurement of peroxyacyl nitrates and dinitrogen pentoxide, *J. Geophys. Res.-Atmos.*, 109, 2004.

Thaler, R. D., Mielke, L. H., and Osthoff, H. D.: Quantification of Nitryl Chloride at Part Per Trillion Mixing Ratios by Thermal Dissociation Cavity Ring-Down Spectroscopy, *Anal. Chem.*, 83, 2761-2766, 2011.

Veres, P., Roberts, J. M., Warneke, C., Welsh-Bon, D., Zahniser, M., Herndon, S., Fall, R., and de Gouw, J.: Development of negative-ion proton-transfer chemical-ionization mass spectrometry (NI-PT-CIMS) for the measurement of gas-phase organic acids in the atmosphere, *International Journal Of Mass Spectrometry*, 274, 48-55, 2008.

Veres, P. R. and Roberts, J. M.: Development of a photochemical source for the production and calibration of acyl peroxy nitrate compounds, *Atmospheric Measurement Techniques*, 8, 2225-2231, 2015.

Wagner, N. L., Dubé, W. P., Washenfelder, R. A., Young, C. J., Pollack, I. B., Ryerson, T. B., and Brown, S. S.: Diode laser-based cavity ring-down instrument for NO₃, N₂O₅, NO, NO₂ and O₃ from aircraft, *Atmos. Meas. Tech.*, 4, 1227-1240, 2011.

Warneke, C., Veres, P., Holloway, J. S., Stutz, J., Tsai, C., Alvarez, S., Rappenglueck, B., Fehsenfeld, F. C., Graus, M., Gilman, J. B., and de Gouw, J. A.: Airborne formaldehyde measurements using PTR-MS: calibration, humidity dependence, inter-comparison and initial results, *Atmospheric Measurement Techniques*, 4, 2345-2358, 2011.

Washenfelder, R. A., Dubé, W. P., Wagner, N. L., and Brown, S. S.: Measurement of atmospheric ozone by cavity ring-down spectroscopy, *Environ. Sci. Technol.*, 45, 2938-2944, 2011a.

Washenfelder, R. A., Langford, A. O., Fuchs, H., and Brown, S. S.: Measurement of glyoxal using an incoherent broadband cavity enhanced absorption spectrometer, *Atmos. Chem. Phys.*, 8, 7779-7793, 2008.

Washenfelder, R. A., Young, C. J., Brown, S. S., Angevine, W. M., Atlas, E. L., Blake, D. R., Bon, D. M., Cubinson, M. J., de Gouw, J. A., Dusanter, S., Flynn, J., Gilman, J. B., Graus, M., Griffith, S., Grossberg, N., Hayes, P. L., Jimenez, J. L., Kuster, W. C., Lefer, B. L., Pollack, I. B., Ryerson, T. B., Stark, H., Stevens, P. S., and Trainer, M. K.: The

glyoxal budget and its contribution to organic aerosol for Los Angeles, California during CalNex 2010, *J. Geophys. Res.*, 116, D00V02, 2011b.

Wild, R. J., Edwards, P. M., Dube, W. P., Baumann, K., Edgerton, E. S., Quinn, P. K., Roberts, J. M., Rollins, A. W., Veres, P. R., Warneke, C., Williams, E. J., Yuan, B., and Brown, S. S.: A Measurement of Total Reactive Nitrogen, NO_y, together with NO₂, NO, and O₃ via Cavity Ring-down Spectroscopy, *Environ. Sci. Technol.*, 48, 9609-9615, 2014.

Wilson, J. C., Lafleur, B. G., Hilbert, H., Seebaugh, W. R., Fox, J., Gesler, D. W., Brock, C. A., Huebert, B. J., and Mullen, J.: Function and performance of a low turbulence inlet for sampling supermicron particles from aircraft platforms, *Aerosol Science and Technology*, 38, 790-802, 2004.

Young, C. J., Washenfelder, R. A., Mielke, L. H., Osthoff, H. D., Veres, P., Cochran, A. K., VandenBoer, T. C., Stark, H., Flynn, J., Grossberg, N., Haman, C. L., Lefer, B., Gilman, J. B., Kuster, W. C., Tsai, C., Pikelnaya, O., Stutz, J., Roberts, J. M., and Brown, S. S.: Vertically resolved measurements of nighttime radical reservoirs in Los Angeles and their contribution to the urban radical budget, *Environ. Sci. Technol.*, in press, 2012.

Zheng, W., Flocke, F. M., Tyndall, G. S., Swanson, A., Orlando, J. J., Roberts, J. M., Huey, L. G., and Tanner, D. J.: Characterization of a thermal decomposition chemical ionization mass spectrometer for the measurement of peroxy acyl nitrates (PANs) in the atmosphere, *Atmos. Chem. Phys.*, 11, 6529-6547, 2011.